

# Self-Assembly of Conjugated Polymers Into Ring Structures by Breath Figures

Yue Wang, Zhongcheng Pan, Juan Peng\*, and Feng Qiu

State Key Laboratory of Molecular Engineering of Polymers, Department of Macromolecular Science, Fudan University, Shanghai 200433, China

## ABSTRACT

A simple method to fabricate rings of conjugated polymers is presented based on the breath figure technique. In humid atmosphere, the rapid evaporation of solvent induces the cooling of the solution surface of conjugated polymers. Water droplets condense onto the solution surface and undergo coalescence to form larger ones. After the solvent and water droplets evaporate completely, isolated rings are formed. Our results show that it is a general method to produce ring structure in different conjugated polymer systems. The influences of solvent properties, solution concentrations, etc. on the pattern formation are investigated. Compared with the conventional honeycomb structure obtained by breath figures, the key to the formation of ring structure is discussed. Furthermore, ring structure can be tuned from circular to elliptic by applying moist air flow with controlled direction onto the surface of the polymer solution. This approach offers a complimentary way to pattern conjugated polymers in a simple, cost-effective, and one-step matter.

**KEYWORDS:** Conjugated Polymer, Breath Figures, Ring Structure, Self-Assembly, Patterning.

## 1. INTRODUCTION

Conjugated polymers have emerged as promising materials for use in electronic devices such as photovoltaic cells, organic field-effect transistors, and light emitting diodes because of their excellent optoelectronic properties and processability.<sup>1</sup> In recent years, various conjugated polymers including poly(*p*-phenylene vinylene) (PPV),<sup>2</sup> poly(3-alkylthiophene) (P3AT),<sup>3</sup> polyfluorene (PF),<sup>4</sup> etc. have been synthesized and extensively investigated. Since the optoelectronic properties of these conjugated polymers are closely related to their structures, controlling their structures by various methods is important for further improvements in device performance. To date, micro- and nanopatterning of conjugated polymers into a desired architecture are mostly based on conventional lithography (photolithography,<sup>5</sup> *e*-beam lithography,<sup>6</sup> etc.) and non-conventional lithography (soft lithography,<sup>7</sup> etc.). Photolithography is the most commonly used technique to fabricate integrated circuits but relatively expensive and can only be directly applicable to limited photosensitive materials. Soft lithography uses a patterned elastomer as the stamp to produce microstructures, which is more convenient. However, fabrication of the patterned elastomer still relies on photolithography. In addition, pattern

distortion usually occurs due to elastomer deformation and it is uneasy to get high resolution registration.

Self-assembly is an alternative approach to organize materials into a variety of ordered or intriguing microscopic structures.<sup>8</sup> Compared with lithographic techniques, the surface patterning by self-assembly is simple and cost-effective. Usually, the preparation of micro- and nanostructured materials involves templating and a variety of templating methods based on self-assembly have emerged including using colloidal crystals,<sup>9</sup> emulsions,<sup>10</sup> surfactants,<sup>11</sup> microphase-separated block copolymers,<sup>12</sup> etc. Since the first report by François et al.<sup>13</sup> a breath figure method, based on evaporative cooling and condensed water droplets, has been widely used to produce ordered honeycomb structures.<sup>14–24</sup> By casting the solution with right nonvolatile solutes and volatile solvent under moist air flow, the solvent evaporation induces the condensation of water droplets, which further self-organizes into a hexagonal template and finally leaves water droplet imprints after the evaporation of solvent and water. This is a single-step self-assembly process, which can be applicable to a diverse of materials.

While many studies have been proceeded based on the breath figure method, and typically 2D or 3D hexagonal honeycomb structures are produced, reports of other structures based on this methodology are limited.<sup>25–28</sup> In this paper, we report the fabrication of self-assembled rings of conjugated polymers based on the breath figure strategy. The ring structures of conjugated polymers have become

\* Author to whom correspondence should be addressed.

Email: [juanpeng@fudan.edu.cn](mailto:juanpeng@fudan.edu.cn)

Received: xx xx xxxx

Accepted: xx xx xxxx

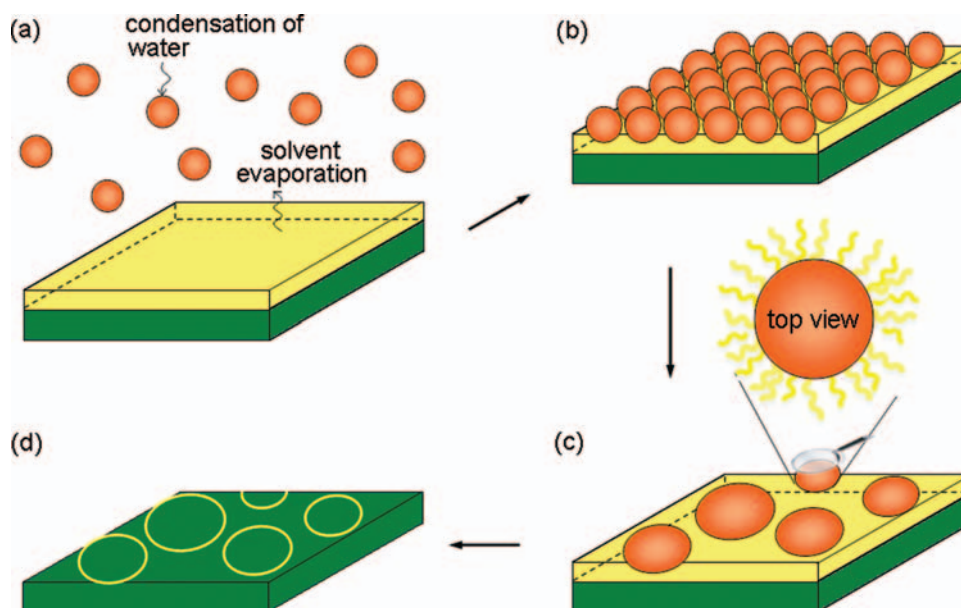


**Fig. 1.** Schematic illustration to the formation of ring structure. (a) Solvent evaporation induces the condensation of water droplets onto the solution surface. (b) Water droplets arrange into hexagonal packing driven by thermocapillary convection. (c) Water droplets coalesce to form larger ones with the precipitation of polymer around the droplets. (d) Ring structure is formed after the evaporation of water droplets and solvent.

attractive because of their special configuration, unique features, and the difficulty in achieving uniformity despite the simplicity in shape. By casting conjugated polymer solutions using volatile solvent under humid atmosphere, water droplets condense onto the solution surface and undergo coalescence to form larger ones. After the evaporation of solvent and water droplets, isolated rings are formed. It is assumed that the stability of condensed water droplets is the key to the formation of ring structure or conventional honeycomb structure. The overall formation process of ring structure is schematically shown in Figure 1.

## 2. EXPERIMENTAL DETAILS

Three conjugated polymers were employed as models including poly[2-methoxy-5-(2-ethylhexyloxy)-1,4-phenylenevinylene] (MEH-PPV,  $M_n = 187300$  g/mol,  $M_w/M_n = 3.68$ ), polyfluorene (PF,  $M_n = 52300$  g/mol,  $M_w/M_n = 2.67$ ), and poly(3-dodecylthiophene) (P3DDT,  $M_n = 10700$  g/mol,  $M_w/M_n = 1.27$ ). The chemical structures of the used conjugated polymers are shown in Figure 2. In a typical experiment, these polymers were dissolved in chloroform ( $\text{CHCl}_3$ ) with concentrations between 0.2 to 10 mg/mL. To investigate the solvent effects on the pattern formation, other solvents including methylene dichloride ( $\text{CH}_2\text{Cl}_2$ ), carbon disulfide ( $\text{CS}_2$ ), carbon tetrachloride ( $\text{CCl}_4$ ), toluene, and tetrahydrofuran (THF) were also used to dissolve these polymers.

For pattern formation, two different methods were used to treat the polymer solution. In most cases without notification, a drop of polymer solution was placed on a carbon-coated copper grid or glass slide and the drop was allowed

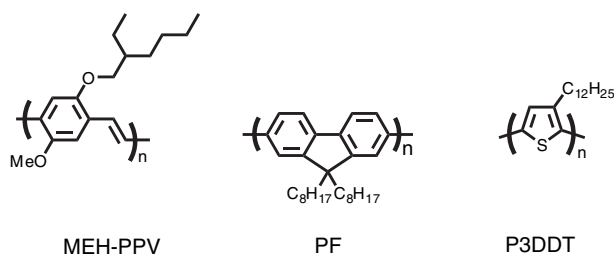


**Fig. 2.** Chemical structures of MEH-PPV, PF, and P3DDT.

to dry in ambient conditions (relative humidity  $\sim 70\%$ ) without using any humidity chamber or air flow. In other cases to increase the humidity or to obtain elliptic rings, moist air flow was sent through a nozzle with controlled direction onto the evaporating surface of the polymer solution (relative humidity  $\sim 90\%$ ). The excess solution was blotted away with filter paper.

After the complete evaporation of solvent, the structure was characterized by transmission electron microscopy (TEM). TEM images were taken on a Tecnai G<sup>2</sup> 20, FEI electron microscope operated at 200 kV accelerating voltage. Confocal laser scanning microscopy was performed on a Leica SP5II, laser scanning confocal microscope. Scanning electron microscopy (SEM) images were taken using a VEGA TS 5136MM instrument operating at 20 kV.

## 3. RESULTS AND DISCUSSION

Figure 3 shows the TEM images of the conjugated polymers MEH-PPV, PF, and P3DDT drop-cast from chloroform solution. Ring-shaped structures were observed in all these systems. TEM at low magnification (Fig. 3(a))

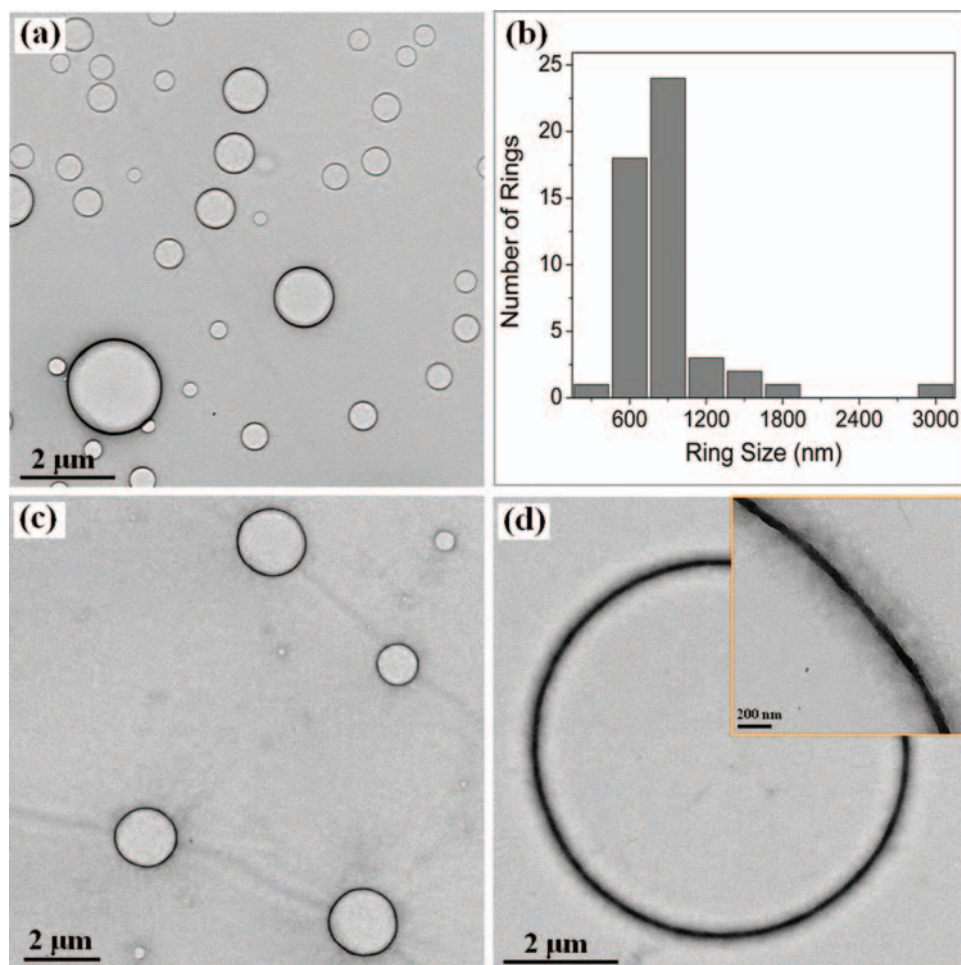


**Fig. 3.** TEM images of rings formed by evaporating different conjugated polymer solutions in chloroform on the carbon-coated grid. (a) MEH-PPV (0.2 mg/mL), (b) size distribution of rings measured from TEM wide fields of (a). (c) PF (3 mg/mL), and (d) P3DDT (1 mg/mL). The inset in (d) is a magnified TEM image of the periphery of a ring.

revealed the ring width typically at  $\sim 110$  nm and the ring sizes ranging from 270 nm to several microns which gave an average value of 750 nm (Fig. 3(b)). The circumference of most rings was clean and clear, but there were a few rings with nanowhiskers attached to their periphery (Fig. 3(d)). The nanowhisker formation was correlated with the nature of P3DDT conjugated polymer, which was involved in a two-step process: (1) coil-to-rod conformational transition of a polymer chain and (2) crystallization of rod-like polymer chains into fibrillar aggregates.<sup>29</sup> Usually, marginal solvent for poly(3-alkylthiophenes) is used to prepare stably dispersed nanowhiskers such as anisole, *p*-xylene, cyclohexanone, and toluene. Although chloroform is a good solvent for P3DDT, nanowhiskers can also be formed as shown in Figure 3(d) due to the decreased solubility of P3DDT when it precipitated around the water droplets. The fine structure within the section of the rings was investigated by high resolution TEM. However, the plan-view image could not provide enough contrast between conjugated polymers and carbon film on the grid (images not shown). The rings were also visible

by confocal laser scanning microscopy, which emitted red light and blue light in MEH-PPV and PF systems, respectively (Fig. 4). Due to the aggregation-induced fluorescent quenching, no fluorescence was observed in the rings of P3DDT.

It is known that the presence of water vapor in the atmosphere is critical and one criterion of the breath figure phenomena.<sup>8</sup> To prove if the ring-shaped structure obtained here was produced by breath figures, a droplet of chloroform solution containing MEH-PPV evaporated in the absence of moisture. In contrast, ring structure was not observed. Therefore, it was concluded that the formation of ring structures, although different from conventional honeycomb structure, conformed to the breath figure mechanism. Besides the humidity of the atmosphere, the presence of nonvolatile solutes, i.e., conjugated polymers in our systems was necessary for the formation of rings. When a drop of pure chloroform without polymers evaporated under the humid atmosphere, nothing was left after the complete evaporation of solvent. Thus, it could be concluded that the conjugated polymers precipitated and

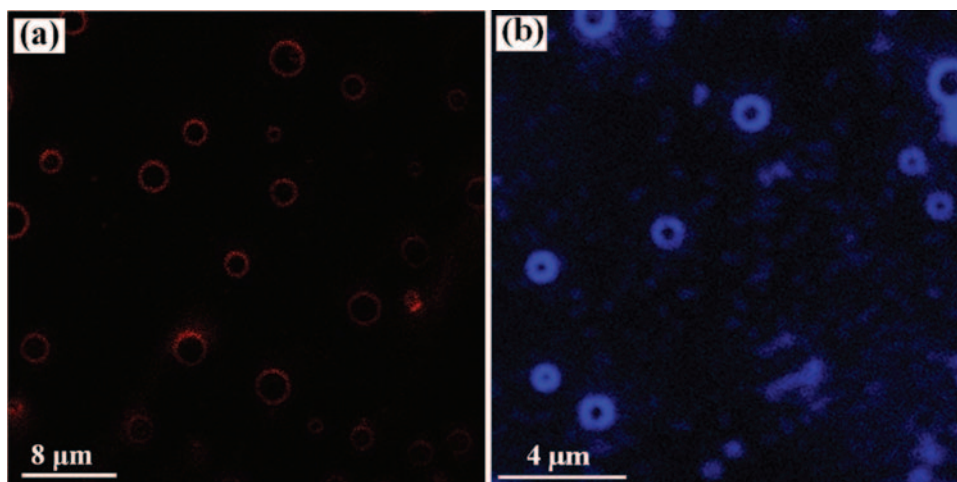


**Fig. 4.** Confocal laser microscopy images of rings formed by evaporating (a) MEH-PPV (1 mg/mL) and (b) PF (0.2 mg/mL) in chloroform on the carbon-coated grid.

trapped the water droplets to protect them from evaporating at the initial stage.

Next we investigated the effect of the solvent on the formation of ring structures. Figure 5 shows TEM images of MEH-PPV in different solvents evaporated on the carbon-coated grid. Similar to the MEH-PPV/chloroform solution, rings could also be prepared in  $\text{CH}_2\text{Cl}_2$ ,  $\text{CS}_2$ , and  $\text{CCl}_4$  systems. Interestingly, in the case of  $\text{CCl}_4$ , each big ring was composed of several small rings close to each other (Fig. 5(c)). When an extra moist airflow was applied to MEH-PPV/ $\text{CCl}_4$  system with a relative humidity of  $\sim 90\%$ , small rings disappeared and only big rings were observed (Fig. 5(d)). However, rings were not found in toluene and THF systems. It is known that the major differences between various solvents are the droplet-solvent interactions and their different evaporation rates which depend mostly on the vapor pressure above the liquid, usually higher vapor pressure leads to faster evaporation. The vapor pressure of chloroform,  $\text{CH}_2\text{Cl}_2$ ,  $\text{CS}_2$ ,  $\text{CCl}_4$ , toluene, and THF at  $20^\circ\text{C}$  is 21.13, 30.15, 39.67, 12.15, 2.91, and 17.28 KPa, respectively.<sup>30</sup> Toluene had the lowest vapor pressure among them thus evaporated the most slowly. The solvents chloroform,  $\text{CH}_2\text{Cl}_2$ ,  $\text{CS}_2$ ,  $\text{CCl}_4$  evaporated very quickly and induced sufficient cooling of the solvent surface rapidly. Therefore, water vapor condensed onto the cold surface of the solution in the form of drops. While toluene could not cool the solvent surface enough to induce the condensation of water droplets, leaving behind flat and featureless polymer films. Although THF had a high vapor pressure which could induce the condensation of water droplets, water and THF were miscible with each other. The condensed water droplets were soon dissolved into THF and thus no rings were formed after the complete evaporation of water and THF. We noticed Khanal et al. had reported that rings could not be formed in hybrid gold/polystyrene core-shell nanorods when toluene and THF were used as solvents.<sup>25</sup> We tried to understand why

there were small rings aggregated in each big ring in  $\text{CCl}_4$  system after the natural evaporation of solvent. A possible explanation was the relatively larger viscosity of  $\text{CCl}_4$  ( $0.978\text{ mPa}\cdot\text{s}$  at  $20^\circ\text{C}$ )<sup>30</sup> led to a more difficult coalescence of adjacent small water droplets into big ones. Therefore, the increase of air humidity in  $\text{CCl}_4$  system was helpful for the coalescence of small water droplets.

At this point, an obvious question arises: What is the decisive factor to determine the formation of ring structure instead of conventional honeycomb structure? Khanal et al. described the assembly of hybrid gold/polystyrene core-shell nanorods into ringlike arrays and attributed the formation of rings to the reduced concentration of solute.<sup>25</sup> Lu et al. fabricated ordered two-dimensional arrays of polymeric rings via a combination of microcontact printing, breath figure technique, and dewetting process, in which the formation of rings was influenced by the solution concentration.<sup>28</sup> Comparing the formation processes of honeycomb structure and ring structure, the key difference is water droplets remain isolated from each other in honeycomb structure while coalescence of water droplets occurs in ring structure. We propose the essence to different structures is the stability of condensed water droplets. We tried to investigate the stability of water droplets by direct observation of their condensation and coalescence via optical microscope. Due to the quick evaporation of solvent, the focus changed quickly and the whole dynamic process could only be observed vaguely. Khanal et al.<sup>25</sup> and Karthaus et al.<sup>21</sup> had directly observed the intermediate process of pure  $\text{CH}_2\text{Cl}_2$  or chloroform evaporating at high humidity and proved the stability of water droplets in pure solvent was poor because no polymers trapped them. Increasing the concentration of polymer solution obviously increased the stability of condensed water droplets. It showed that ring-shaped structure was formed in P3DDT chloroform solution with the concentration of 1 mg/mL (Fig. 6(a)). When the concentration of P3DDT solution

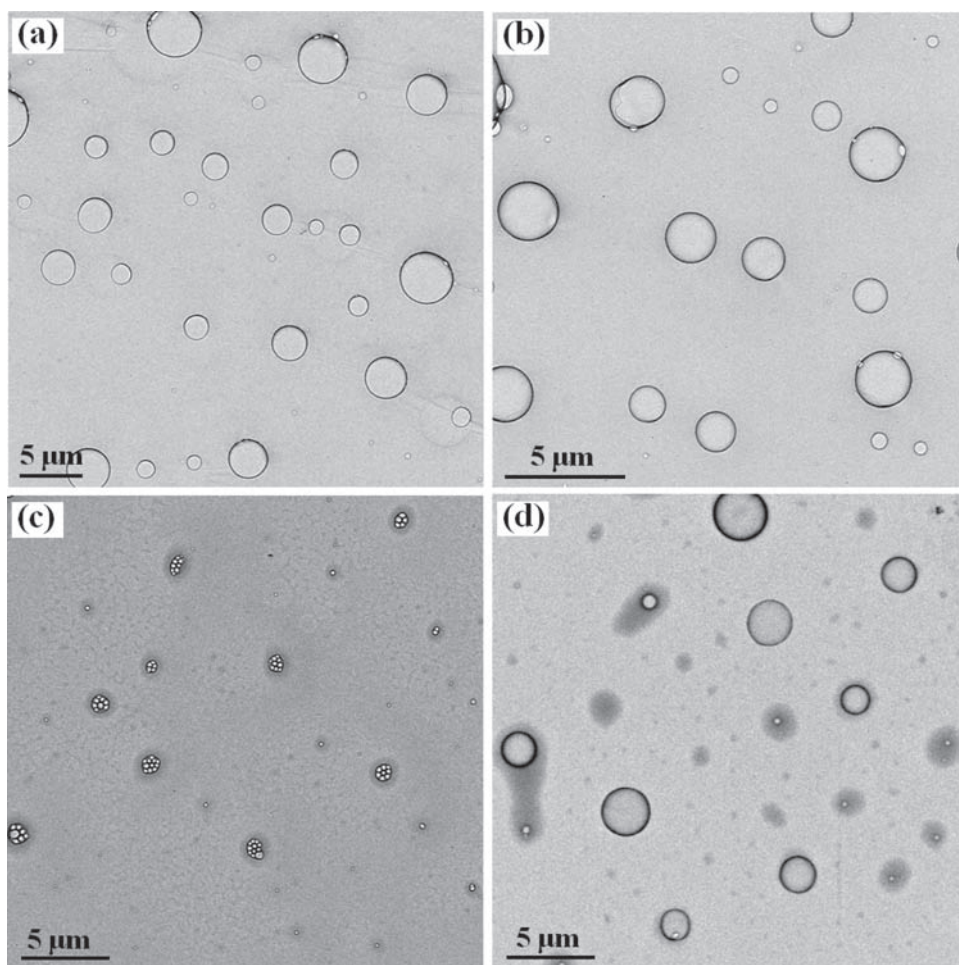


**Fig. 5.** TEM images of rings formed by evaporating MEH-PPV solutions of different solvents (1 mg/mL) on the carbon-coated grid. (a)  $\text{CH}_2\text{Cl}_2$ , (b)  $\text{CS}_2$ , and (c) and (d)  $\text{CCl}_4$ . (d) An extra moist airflow was applied to MEH-PPV/ $\text{CCl}_4$  system with a relative humidity of  $\sim 90\%$ .

was increased to 5 mg/mL, highly ordered honeycomb structure was obtained (Fig. 6(b)). Further increasing the concentration of P3DDT (10 mg/mL) led to the formation of multilayer honeycomb structure (Fig. 6(c)). The concentration of polymer solution determined the solution viscosity upon other uniform conditions.<sup>31</sup> When the

solution viscosity was comparably low, the stability of condensed water droplets was low. The conjugated polymer precipitated around the water droplets to protect them from going out of solution surface at the initial stage, but could not prevent them from coalescence to form larger ones. After the evaporation of solvent and water droplets,

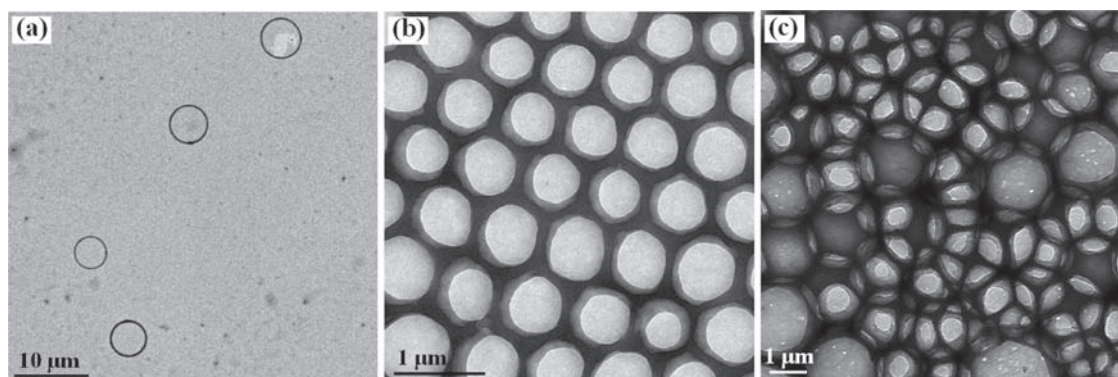


**Fig. 6.** TEM images of nanostructures formed by evaporating P3DDT chloroform solutions with different concentrations on the carbon-coated grid. (a) 1 mg/mL, (b) 5 mg/mL, and (c) 10 mg/mL.

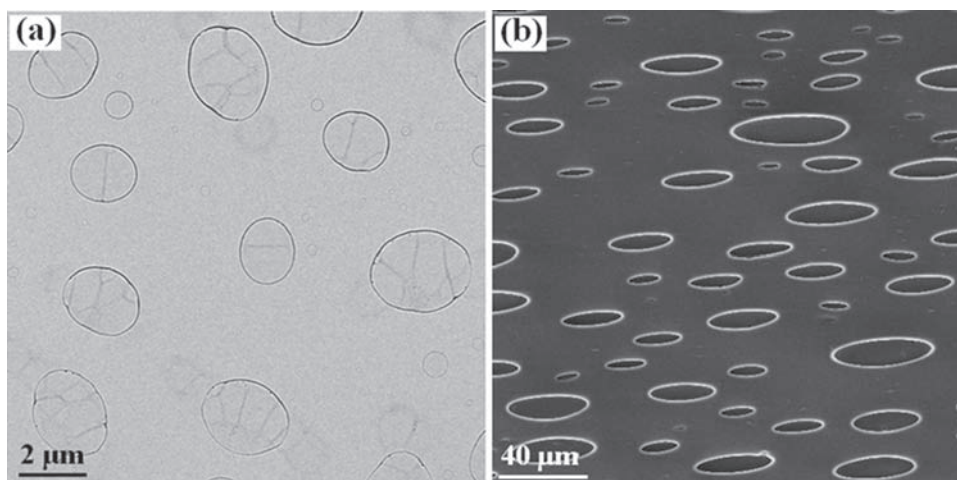


**Fig. 7.** (a) TEM and (b) SEM images of elliptic rings formed by evaporating MEH-PPV chloroform solution on the carbon-coated grid and glass slide, respectively. The concentration of MEH-PPV solution is (a) 1 mg/mL and (b) 5 mg/mL, respectively. Moist air flow was sent through a nozzle with controlled direction onto the evaporating surface of the polymer solution.

ring structure was produced. When a certain concentration with appropriate solution viscosity was achieved, the trapped droplets were stabilized by the precipitated polymers, which further self-assembled into hexagonal arrays, leaving behind conventional honeycomb structure. When the concentration was high, the solution was viscous thus the trapped droplets could not rearrange themselves due to resistance before more droplets condensed onto them, leading to multilayer honeycomb structures. During the process of solvent evaporation, the thermocapillary current driven by the temperature gradient between the solution surface and the substrate may also help the formation of multilayer honeycomb structures.

Interestingly, we showed that the ring structure could be tuned from circular to elliptic by applying an extra moist air flow with controlled direction onto the evaporating surface of the polymer solution (Fig. 7). We have previously reported the first example of hexagonal array of elliptic pores in gold nanoparticle films by breath figure method.<sup>24</sup> The formation process of the elliptic rings was similar to the hexagonal array of elliptic pores. The moist air flow was used to increase the environmental humidity and deform the shape of condensed water droplets into elongated ellipsoid via additional shear force. After the evaporation of solvent and water droplets, elliptic rings were formed. It showed that elliptic rings with random direction were formed in MEH-PPV chloroform solution with the concentration of 1 mg/mL (Fig. 7(a)). Because the concentration and viscosity of the solution was low, the deformed droplets turned round with random direction during the evaporation process. We noted some small rings remained circular in this case. When increasing the concentration of MEH-PPV solution to 5 mg/mL, elliptic structures with much larger aspect ratio and controlled direction were formed (Fig. 7(b)).

#### 4. CONCLUSION

In summary, breath figure method has been intensively investigated to obtain honeycomb structure of water droplet imprints. In our work, we used it as a tool to produce isolated ring structure in different conjugated polymers. The effects of solvent properties, solution concentrations, etc. on the pattern formation were investigated and the formation mechanism of the ring structure was proposed. The stability of condensed water droplets was found to be a key factor to determine the ring structure or conventional honeycomb structure. The ring structure could be tuned from circular to elliptic by applying moist air flow with controlled direction onto the surface of the polymer solution. In contrast to the multistep patterning of conjugated polymers, the present method was a single-step self-organization process for the preparation of ring structures, thus providing a complimentary strategy to patterning techniques.

**Acknowledgment:** This work was financially supported by the National Natural Science Foundation of China (Grant Nos. 21074026 and 21274029) and National Basic Research Program of China (2011CB605700).

#### References and Notes

1. A. C. Arias, J. D. Mackenzie, I. McCulloch, J. Rivnay, and A. Salleo, *Chem. Rev.* 110, 3 (2010).
2. S. J. Lim, D. Y. Seok, B. K. An, S. D. Jung, and S. Y. Park, *Macromolecules* 39, 9 (2006).
3. R. J. Kline, M. D. McGehee, E. N. Kadnikova, J. Liu, and J. M. J. Fréchet, *Adv. Mater.* 15, 1519 (2003).
4. G. Zhou, G. Qian, L. Ma, Y. Cheng, Z. Xie, L. Wang, X. Jing, and F. Wang, *Macromolecules* 38, 5416 (2005).
5. T. Cao, F. Wei, X. Jiao, J. Chen, W. Liao, X. Zhao, and W. Cao, *Langmuir* 19, 8127 (2003).
6. Z. Pan, S. K. Donthu, N. Wu, S. Li, and V. P. Dravid, *Small* 2, 274 (2006).

7. Y. Xia and G. M. Whitesides, *Annu. Rev. Mater. Sci.* 28, 153 (1998).
8. H. Ma and J. Hao, *Chem. Soc. Rev.* 40, 5457 (2011).
9. O. D. Velev and E. W. Kaler, *Adv. Mater.* 12, 531 (2000).
10. A. Imhof and D. J. Pine, *Nature* 389, 948 (1997).
11. M. Antonietti, *Curr. Opin. Colloid Interface Sci.* 6, 244 (2001).
12. J. Y. Cheng, C. A. Ross, H. I. Smith, and E. L. Thomas, *Adv. Mater.* 18, 2505 (2006).
13. G. Widawski, M. Rawiso, and B. François, *Nature* 369, 387 (1994).
14. M. Srinivasarao, D. Collings, A. Philips, and S. Patel, *Science* 292, 79 (2001).
15. L. Song, R. K. Bly, J. N. Wilson, S. Bakbak, J. O. Park, M. Srinivasarao, and U. H. F. Bunz, *Adv. Mater.* 16, 115 (2004).
16. G. Vamvounis, D. Nyström, P. Antoni, M. Lindgren, S. Holdcroft, and A. Hult, *Langmuir* 22, 3959 (2006).
17. U. H. F. Bunz, *Adv. Mater.* 18, 973 (2006).
18. V. Vohra, S. Yunus, A. Attout, U. Giovanella, G. Scavia, R. Tubino, C. Botta, and A. Bolognesi, *Soft Matter* 5, 1656 (2009).
19. S. H. Lee, J. S. Park, B. K. Lim, C. B. Mo, W. J. Lee, J. M. Lee, S. H. Hong, and S. O. Kim, *Soft Matter* 5, 2343 (2009).
20. Y. C. Chiu, C. C. Kuo, C. J. Lin, and W. C. Chen, *Soft Matter* 7, 9350 (2011).
21. O. Karthaus, N. Maruyama, X. Cieren, M. Shimomura, H. Hasegawa, and T. Hashimoto, *Langmuir* 16, 6071 (2000).
22. A. Böker, Y. Lin, K. Chiapperini, R. Horowitz, M. Thompson, V. Carreon, T. Xu, C. Abetz, H. Skaff, A. D. Dinsmore, T. Emrick, and T. P. Russell, *Nat. Mater.* 3, 302 (2004).
23. J. Peng, Y. Han, J. Fu, Y. Yang, and B. Li, *Macromol. Chem. Phys.* 204, 125 (2003).
24. J. Li, J. Peng, W. Huang, Y. Wu, J. Fu, Y. Cong, L. Xue, and Y. Han, *Langmuir* 21, 2017 (2005).
25. B. P. Khanal and E. R. Zubarev, *Angew. Chem. Int. Ed.* 46, 2195 (2007).
26. L. Zhang, H. Y. Si, and H. L. Zhang, *J. Mater. Chem.* 18, 2660 (2008).
27. J. Gómez-Segura, O. Kazakova, J. Davies, P. Josephs-Franks, J. Veciana, and D. Ruiz-Molina, *Chem. Commun.* 45, 5615 (2005).
28. G. Lu, W. Li, J. Yao, G. Zhang, B. Yang, and J. Shen, *Adv. Mater.* 14, 1049 (2002).
29. S. Samitsu, T. Shimomura, S. Heike, T. Hashizume, and K. Ito, *Macromolecules* 41, 8000 (2008).
30. G. Q. Liu, L. X. Ma, and J. Liu (eds.), *Chemical Property Data Handbook*, Chemical Industry Press, Beijing, China (2002).
31. J. Peng, Y. Han, Y. Yang, and B. Li, *Polymer* 45, 447 (2004).